Acknowledgment. This research was supported in part by grants from the NIH, CA-50679 and HL-33550, the Balaban Foundation, the Council for Tabacco Research-USA, Inc., and the NSF, The Chemistry of Life Sciences Program, DCB-8616115. We acknowledge the useful comments of Michael K. Bowman of the Argonne National Laboratory and the assistance of Becky Nyquist of the University of Chicago.

Supplementary Material Available: Description of calculations, tables of NMR data derived from the Breit-Rabi Hamiltonian equation for compounds IV-IX, and figures showing the low modulation amplitude spectra and spectral simulations of the superoxide adducts of compounds IV-VI and the hydroxyl adduct of compound IX (13 pages). Ordering information is given on any current masthead page.

Electronic Transition Moment Directions and Identification of Low-Energy $n\pi^*$ States in Weakly Perturbed Purine Chromophores

Bo Albinsson* and Bengt Nordén

Contribution from the Department of Physical Chemistry, Chalmers University of Technology, 412 96 Göteborg, Sweden. *Received April 6, 1992*

Abstract: Measurements of UV linear dichroism on purine and three methyl derivatives partially oriented in poly(vinyl alcohol) matrix gave direct evidence for the assignment of the first singlet $n\pi^*$ state. Intensity distributions and moment directions for the first three $\pi \rightarrow \pi^*$ transitions were also determined. The $\pi \rightarrow \pi^*$ transitions in purine were found to be polarized at (angles, relative to the pseudo-symmetry long axis, counted positive in the N7 direction): $-31° \pm 5°$ (II at 265 nm), $+38° \pm 5°$ (III at 244 nm), and $+36° \pm 10°$ (IV at 214 nm). The transition energies and moment directions were not markedly perturbed by methyl substitution at the sixth, seventh, or ninth position. Therefore, these methyl substituents could be used as *orientational* perturbers to resolve a sign ambiguity problem regarding transition moment directions. The orientation parameters were determined by infrared dichroic measurements using both in-plane and out-of-plane polarized vibrational transitions. In addition, the phosphorescence spectra were studied, including phosphorescence anisotropy, phosphorescence lifetimes, and quantum yields, for the purines in an organic glass at 80 K. Based on these measurements, the lowest triplet state is concluded to have effectively $\pi\pi^*$ character, and its emission allowedness appears to originate from spin-orbit interactions primarily with singlet $\sigma\pi^*$ states but also with singlet $\pi\pi^*$ states via vibronic mixing. The phosphorescence emission spectra of purine and 6-methylpurine are complex, compared to 7-methylpurine and 9-methylpurine, with emission wavelength-dependent lifetimes and excitation spectra. This is ascribed to a prototropic tautomeric equilibrium between the 7H and 9H forms of purine and 6-methylpurine, a ground-state heterogeneity that we believe has caused confusion in earlier studies and, e.g., led to an incorrect assignment of the phosphorescence origin of purine.

Introduction

Excited-state properties of the purine chromophore are of utmost importance for understanding the spectroscopy of nucleic acids. Many questions are still to be resolved such as those concerning the unexpected low emission yields of the DNA bases and the potential influence of the $n\pi^*$ states. A number of investigations have been performed to understand the primary processes lowering the quantum yields for emission in the purine bases. The emerging picture is that very fast internal conversion ($k_{ic} = 10^{11}-10^{12}$ s^{-1}) efficiently competes with the radiative processes even at liquid nitrogen temperature,[1,2] but no detailed description of the quenching process has so far been given. The energy order of the excited states of the purine chromophore is very sensitive to electron-donating substituents at certain positions, which makes the emission properties highly sensitive in this respect. Near degeneracy of the $n\pi^*$ and $\pi\pi^*$ states has been proposed to increase internal conversion in N-heterocyclic systems,[3,4] and, thus, a detailed knowledge of the lowest excited states would be expected to become a key parameter to understand the photophysics of the purine bases.

Purine is a logical model chromophore for the nucleic acid bases adenine and guanine. Theoretical correlation between the excited states of purine and the nucleic acid bases has been proposed by Hug and Tinoco.[5] They calculated the transition monopoles and used the nodal properties of the wave functions to identify and characterize the different electronic transitions. Callis has extended their approach to include off-diagonal terms in the transition density matrix[6,7] and thereby found large similarities between adenine and purine, but not between guanine and purine, for the two lowest $\pi \rightarrow \pi^*$ transitions. In spite of the key roll of purine in various contexts, only a few experimental studies have been reported. Cohen and Goodman from phosphorescence and polarized phosphorescence spectra on purine made an indirect $n\pi^*$ assignment of the lowest excited state.[8] Drobnik et al. addressed several important questions on the solvent and substitution sensitivity of the purine electronic states.[9-12] They found evidence for an $n\pi^*$ state to be lowest in energy and argued for two $\pi \rightarrow \pi^*$ transitions in the 260-nm band. Chen and Clark performed a polarized reflection study on purine crystals[13] and calculated

(1) Eisinger, J.; Lamola, A. A. In *Excited States of Proteins and Nucleic Acids*; Steiner, R. F., Weinryb, I., Eds.; Plenum Press: New York, 1971.
(2) Callis, P. R. *Annu. Rev. Phys. Chem.* **1983**, *34*, 329-357.
(3) Lim, E. C. *J. Phys. Chem.* **1986**, *90*, 6770-6777.
(4) Wassan, W. A.; Lim, E. C. *Chem. Phys.* **1980**, *48*, 299-305.
(5) Hug, W.; Tinoco, I., Jr. *J. Am. Chem. Soc.* **1973**, *95*, 2803-2813.
(6) Callis, P. R. *Photochem. Photobiol.* **1986**, *44*, 315-332.
(7) Callis, P. R. *Int. J. Quantum Chem., Quantum Chem. Symp.* **1984**, *18*, 579-588.
(8) Cohen, B. J.; Goodman, L. *J. Am. Chem. Soc.* **1965**, *87*, 5487-5490.
(9) Drobnik, J.; Augenstein, L. *Photochem. Photobiol.* **1966**, *5*, 13-30.
(10) Drobnik, J.; Augenstein, L. *Photochem. Photobiol.* **1966**, *5*, 83-97.
(11) Kleinwächter, V.; Drobnik, J.; Augenstein, L. *Photochem. Photobiol.* **1967**, *6*, 133-146.
(12) Drobnik, J.; Kleinwächter, V.; Augenstein, L. *Photochem. Photobiol.* **1967**, *6*, 147-154.
(13) Chen, H. H.; Clark, L. B. *J. Chem. Phys.* **1969**, *51*, 1862-1871.

0002-7863/93/1515-223$04.00/0

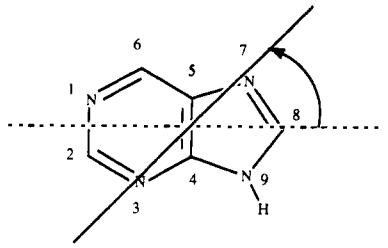

Purine

Figure 1. Purine chromophore with substituent positions and definition of an in-plane angle relative to the pseudo-symmetry long axis.

the polarized absorption spectrum with and without taking crystal fields into account. The 260-nm band is, according to these authors, composed of an in-plane polarized $\pi \rightarrow \pi^*$ transition at 265 nm and a strong out-of-plane polarized $n \rightarrow \pi^*$ transition at 240 nm,[13] at variance with the polarized phosphorescence results.[8,12]

Another interesting, sometimes annoying, property of the purine bases is the possibility of tautomeric equilibria. In purine the imidazolic hydrogen is the only likely candidate, whereas in the DNA bases guanine and adenine additional tautomers, including keto–enol and amine–imine forms, are possible. Purine exists in the 7H form (Figure 1) in the crystal structure,[14] whereas the 9H form predominates for adenine in the gas phase,[15] and purine isolated in the noble gas matrix,[16] and this is the stable form according to quantum mechanical calculations.[17] In fluid solution the two prototropic tautomers of purine exist in varying amounts depending on polarity of solvent, as judged from ^{13}C-NMR[18,19] and ^{15}N-NMR[20] shifts. The temperature dependence of this equilibrium has, to our knowledge, not been studied.

This article presents polarized absorption measurements on purine, 6-methylpurine, 7-methylpurine, and 9-methylpurine oriented in a stretched poly(vinyl alcohol) polymer, a medium where the concentration of the solute is kept low, thereby minimizing exciton interaction. Monomeric spectra are important in experimental as well as theoretical contexts, and, in fact, dramatic effects of crystal fields have recently been shown to be a problem with nucleic acid bases.[21] The purine derivatives were chosen from three viewpoints: (1) to isolate possible tautomeric forms, (2) to introduce orientational perturbations in order to resolve the absolute transition moment directions, and, (3) to introduce weak electronic perturbations at specific sites on the purine chromophoric core. The orientational properties of the chromophores in the polymeric host are determined by measurements of polarized IR spectra. We have also measured emission spectra and correlated emission properties to the characterization of the excited states. This is particularly important when comparing more strongly perturbed purine systems where, as mentioned, quite different and puzzling emission properties are encountered. In a following publication, the electronic states and emission properties of amino- and methoxy-substituted purines are investigated.[22] In addition, a ground-state heterogeneity, presumably due to prototropic tautomers, results in complex phosphorescence spectra of purine and 6-methylpurine at 80 K. The experimental findings are finally compared with the results from a standard semiempirical molecular orbital calculation.

Materials and Methods

Chemicals. Purine and 6-methylpurine (6MP) were purchased from Sigma and used without further purification. 7- and 9-methylpurine (7MP and 9MP) were synthesized by methylation of purine with methyl iodide using sodium hydride as a base.[20] The two isomers were separated on a silica column with ethanol/water (95/5) as elutant and recrystallized twice from hot benzene solution. All solvents (ethanol, diethyl ether, and 2-methylbutane) showed small or negligible emissive impurities and were used directly from the bottles. The poly(vinyl alcohol) (PVA) powder from E. I. du Pont de Nemours and Co. (Elvanol 71-30) was refluxed for 6 h in alkaline 50% ethanol, to hydrolyze residual acetate and thereafter washed in 95% ethanol. PVA was mixed with cold water (10% w/v) and dissolved by heating to 90 °C under vigorous stirring. Aliquots of 5 mL were mixed with 3 mL of aqueous solution of each of the compounds yielding final concentrations in the range 0.1–10 mM. The solutions were gently poured onto the glass plates and left to dry in a dust-free environment for at least 24 h. The films were then removed with a spatula and stretched mechanically at an elevated temperature (80 °C) to an extension factor of 5.

Linear dichroism (LD) at a given wavelength (λ) is defined as

$$\mathrm{LD}(\lambda) = A_{\parallel}(\lambda) - A_{\perp}(\lambda) \quad (1)$$

where $A_{\parallel}$ and $A_{\perp}$ are the absorbances measured with plane polarized light with the polarization parallel and perpendicular to the unique sample axis (the stretching direction of the film). The reduced linear dichroism (LD^r) is

$$\mathrm{LD}^r(\lambda) = \mathrm{LD}(\lambda)/A_{\mathrm{iso}}(\lambda) \quad (2)$$

where A_{iso} is the absorbance of a corresponding isotropic sample. For a uniaxially oriented sample, such as the PVA film, the isotropic absorbance can be calculated from the polarized components as[23]

$$A_{\mathrm{iso}} = \tfrac{1}{3}(A_{\parallel} + 2A_{\perp}) \quad (3)$$

The LD^r of a pure in-plane polarized transition i in a chromophore such as purine with C_s symmetry (having only a plane of symmetry) is related to the angle (θ_i) between a transition moment, polarized in the plane of the molecule, and the preferred molecular orientation axis (z) according to[24]

$$\mathrm{LD}^r_i = 3(S_{zz}\cos^2\theta_i + S_{yy}\sin^2\theta_i) \quad (4)$$

where S_{zz} and S_{yy} are respectively the Saupe orientation parameters for the in-plane (diagonal) axes z and y.[25] The LD^r of any out-of-plane polarized transition is equal to the orientation parameter for the out-of-plane axis x multiplied by 3:

$$\mathrm{LD}^r_x = 3S_{xx} \quad (5)$$

For in-plane polarized transitions the LD^r can take values between $3S_{yy}$ and $3S_{zz}$ according to eq 4.

$$3S_{yy} \le \mathrm{LD}^r(\text{in-plane}) \le 3S_{zz} \quad (6)$$

The orientation parameters are quadratic functions of directional cosines and are interrelated according to

$$S_{xx} + S_{yy} + S_{zz} = 0 \quad (7)$$

For overlapping transitions the observed LD^r is a weighted average of the LD^r_i values of the contributing transitions[26]

$$\mathrm{LD}^r(\lambda) = \sum_i A_i(\lambda)\mathrm{LD}^r_i / \sum_i A_i(\lambda) \quad (8)$$

where $A_i(\lambda)$ is the absorbance associated with transition i. The "pure" reduced linear dichroism LD^r_i is obtained either by a curve-fitting procedure described below or from the experiments by a trial-and-error method ("TEM")[27,28] based on the stepwise formation of linear combinations of the polarized spectra (e.g., $A_{\parallel}(\lambda) - d_i A_{\perp}(\lambda)$). The subtraction coefficient (d_i), for which a specific spectral feature disappears in the

(14) Watson, D. G.; Sweet, R. M.; Marsh, R. E. *Acta Crystallogr.* **1965**, *19*, 573–580.
(15) Peng, S.; Padra, A.; LeBreton, P. R. *Proc. Natl. Acad. Sci. U.S.A.* **1976**, *US73*, 2966–2968.
(16) Nowak, M. J.; Lapinski, L.; Kwiatowski, J. S. *Chem. Phys. Lett.* **1989**, *157*, 14–18.
(17) Nowak, M. J.; Lapinski, L.; Kwiatowski, J. S.; Leszczynski, J. *Spectrochim. Acta* **1991**, *47A*, 87–103.
(18) Chenon, M.-T.; Pugmire, R. J.; Grant, D. M.; Panzica, R. P.; Townsend, L. R. *J. Am. Chem. Soc.* **1975**, *97*, 4636–4642.
(19) Schumacher, M.; Günter, H. *J. Am. Chem. Soc.* **1982**, *104*, 4167–4173.
(20) Gonella, N. C.; Roberts, J. D. *J. Am. Chem. Soc.* **1982**, *104*, 3162–3164.
(21) Theiste, D.; Callis, P. R.; Woody, R. W. *J. Am. Chem. Soc.* **1991**, *113*, 3260–3267.
(22) Albinsson, B.; Nordén, B. Work in progress.
(23) Michl, J.; Thulstrup, E. W. *Spectroscopy with Polarized Light*; VCH Publishers: New York, 1986.
(24) Matsouka, Y.; Nordén, B. *J. Phys. Chem.* **1982**, *86*, 1378–1386.
(25) Saupe, A. *Mol. Cryst.* **1966**, *1*, 527–540.
(26) Nordén, B. *Appl. Spectrosc. Rev.* **1978**, *14*, 157–248.
(27) Thulstrup, E. W.; Michl, J.; Eggers, J. H. *J. Phys. Chem.* **1970**, *74*, 3868–3878.
(28) Michl, J.; Thulstrup, E. W.; Eggers, J. H. *J. Phys. Chem.* **1970**, *74*, 3878–3884.

linear combination, is related to the LD^r_i of the transition containing that feature[29a]

$$LD^r_i = 3\frac{d_i - 1}{d_i + 2} \tag{9}$$

The UV spectra of purine derivatives in polar environment shows very little structural resolution and the TEM method is, therefore, in this case, of limited use. Instead the polarized spectra are fitted to Gaussian profiles with equal center wavelengths and band widths but with different amplitudes for the two components, from which the intrinsic LD^r values are calculated. The number of Gaussians is chosen so as to describe the intensity distribution as well as polarization variations with wavelength.

Polarized IR measurements were performed on a Perkin-Elmer 1800 Fourier transform spectrometer equipped with a KRS-5 polarizer (IGP228 Cambridge Physical Science). The nominal resolution was 2 cm^{-1} and each spectrum was an average over 100 scans. A base line for PVA was recorded similarly and subtracted on an interfaced computer. The LD^r_i values were evaluated with respect to peak heights and peak areas. The parallel and perpendicular components were also linearly combined according to the TEM method which proved particularly useful to resolve solute peaks in the presence of a strongly wavelength-dependent PVA base line.

Polarized UV measurements were performed on a Cary 2300 spectrophotometer equipped with two rotatable Glan air-space calcite polarizers in sample and reference beams. The spectrophotometer was interfaced with a computer, and five data points per nanometer were collected at a spectral band width of 1 nm. The LD^r_i values provide measures of the orientation of the transition moments relative to the molecular axis that is on the average best aligned, i.e., the orientation axis z. For a particular molecule the LD^r can, for in-plane polarized transitions, vary between $3S_{yy}$ and $3S_{zz}$ according to eq 6. An in-plane transition moment oriented perpendicular to the orientation axis shows a small LD^r value, and a transition polarized close to the orientation axis shows a large LD^r value. Given the orientation parameters and the direction of the orientation axis z, the polarizations of the UV transition moments were calculated by use of eq 4. The angle θ_i was transformed into an angle δ_i within the molecular framework by adding or subtracting to the angle (α) that specifies the direction of the orientation axis:

$$\delta_i = \alpha \pm |\theta_i| \tag{10}$$

where δ_i and α are the angles from the pseudo-symmetry long axis of the indole chromophore to the transition dipole moment and the orientation axis, respectively.

Emission measurements were performed on an AMINCO SPF-500 "corrected spectra" spectrofluorimeter. For polarized measurements the spectrofluorimeter was equipped with a Glan polarizer for UV excitation and a Polaroid film in the emitted beam. The emission was measured with 2-nm spectral resolution, and the excitation was either at 264 nm with 2-nm band-pass or at 290 nm with 4-nm band-pass. Solutions of sample substance (approximately 0.2 mM in 99% ethanol or in a 5:5:2 mixture of diethyl ether, 2-methylbutane, and ethanol, EPA) were prepared immediately before use, and the emission was measured at 80 K in a thermostated nitrogen dewar. The relative quantum yields were measured accurately relative to a weakly fluorescent impurity in the ether solvent. This impurity did not affect the measured phosphorescence but proved very useful as an internal standard to obtain relative emission intensities. The "absolute" phosphorescence quantum yield was determined for purine in EPA at 80 K relative to the fluorescence of 9,10-diphenylanthracene (DPA) in EPA at 80 K assuming $\Phi_f = 1$ (the fluorescence quantum yield of DPA in cyclohexane at room temperature is $\Phi_f = 0.9$).[29b] The phosphorescence lifetime was measured by shutting the excitation beam and recording the decay on a time-calibrated XY-recorder. The instrumental response time was estimated to be faster than 0.1 s. The polarized intensities were measured with polarizers set either vertically (v) or horizontally (h) in the excitation and emission light beams. The degree of anisotropy, r, was calculated as

$$r = \frac{I_{vv} - I_{vh}G}{I_{vv} + 2I_{vh}G} \tag{11}$$

where $G = I_{hv}/I_{hh}$ provides instrumental correction. In the subscript of I, the first letter refers to the excitation polarizer and the second to the emission polarizer. The anisotropy, of a non-rotating molecule, the limiting anisotropy, r_0, is related to the angle (ξ) between the absorbing and emitting transition moments:[30]

$$r_0 = (3\cos^2\xi - 1)/5 \tag{12}$$

and thus, varies between +0.4 for parallel transition moments and −0.2 for perpendicular moments. Phosphorescence excitation spectra were measured on samples with total absorbances below 0.1 in order to minimize the influence of absorption on spectral band shape (inner filter effect).

Quantum Mechanical Calculations. The CNDO/S molecular orbital calculations were carried out using a standard program[31-35] where the two-center electron repulsion integrals were approximated by the Mataga–Nishimoto scheme.[36] The molecular geometry was assumed to be described sufficiently accurate for our purposes by a regular hexagon and pentagon using atomic distances; $R_{CC} = R_{CN} = 1.4$ Å, $R_{CH} = R_{NH} = 1.05$ Å. Purine and 6-methylpurine were assumed to be in the 9H tautomeric form. The presented calculations were based on only 20 singly excited configurations, although a larger CI basis set (up to 200 singly excited configurations) was also tested; however, without any significant improvement of the results.

Results

Linear Dichroism. Purine and its methyl derivatives show two major absorption regions above 200 nm. The first, centered around 260 nm, consists of two in-plane polarized $\pi \rightarrow \pi^*$ transitions and one out-of-plane polarized $n \rightarrow \pi^*$ transition at the red edge of the band.[37] To the second absorption band around 205 nm at least two in-plane polarized $\pi \rightarrow \pi^*$ transitions contribute.[38] Figure 2 shows UV absorption and reduced linear dichroism (LD^r) spectra for purine, 6-methylpurine, 7-methylpurine, and 9-methylpurine in stretched poly(vinyl alcohol) films. The spectra are resolved into five Gaussian components where the parallel and perpendicular components are fitted simultaneously with the same center frequencies and band widths. By this procedure both the absorption features as well as the variation in polarization are taken into account, and the intrinsic LD^r for each transition is calculated from amplitudes of the parallel and perpendicular components using eqs 2 and 3. The LD^r calculated from the fitted absorption components, shown for purine as a representative example (top panel of Figure 2), generally decreases toward more negative values, in the red tail of the absorption, than the experimental curve, a deviation that will be explained in the Discussion.

In order to evaluate transition moment directions from LD^r values, the orientational properties of the solute molecules must be known. The orientation, for our purposes, is sufficiently described by two orientation parameters and the direction of the orientation axis. For "small" molecules oriented in polymeric hosts (polyethylene and poly(vinyl alcohol)), measurements of polarized IR spectra have in a number of cases provided enough information to calculate these entities.[39,40] Figure 3 shows the polarized IR spectrum for 9-methylpurine (in the readily measurable range 1800–450 cm^{-1}) and the evaluated LD^r values. Table I comprises the data evaluated from the polarized spectra for purine, 6-methylpurine, 7-methylpurine, and 9-methylpurine together with assignments for purine in H_2O.[41] The "exact" solution is available if three or more IR transition moment directions are known. For purine and its methyl derivatives, only the out-of-plane polarized transitions have a priori known directions and thereby provide a value for the out-of-plane orientation parameter, S_{xx}. One of the in-plane orientation parameters, S_{zz} and S_{yy}, is estimated from the maximum or minimum LD^r values of all the in-plane transitions, and the remaining parameter is calculated from eq 7. The

(29) (a) Albinsson, B.; Kubista, M.; Sandros, K.; Norden, B. *J. Phys. Chem.* **1990**, *94*, 4006–4011. (b) Hamai, S.; Hirayama, F. *J. Phys. Chem.* **1983**, *87*, 83.

(30) Cantor, R. C.; Schimmel, P. R. *Biophysical Chemistry*; W. H. Freeman: San Francisco, 1980; Vol. II, pp 409–480.

(31) Pople, J. A.; Santzy, D. P.; Segal, G. A. *J. Chem. Phys.* **1965**, *43*, S129–S151.

(32) Delbene, J.; Jaffe, H. H. *J. Chem. Phys.* **1968**, *48*, 1807–1813.

(33) Delbene, J.; Jaffe, H. H. *J. Chem. Phys.* **1968**, *48*, 4050–4055.

(34) Delbene, J.; Jaffe, H. H. *J. Chem. Phys.* **1968**, *49*, 1221–1229.

(35) Delbene, J.; Jaffe, H. H. *J. Chem. Phys.* **1969**, *50*, 1126–1129.

(36) Nishimoto, K.; Mataga, N. *Z. Phys. Chem.* **1957**, *12*, 335–338.

(37) Clark, L. B.; Tinoco, I., Jr. *J. Am. Chem. Soc.* **1965**, *87*, 11–15.

(38) Mason, S. F. *J. Chem. Soc.* **1954**, 2071–2081.

(39) Albinsson, B.; Kubista, M.; Nordén, B.; Thulstrup, E. W. *J. Phys. Chem.* **1989**, *93*, 6646–6654.

(40) Albinsson, B.; Nordén, B. *J. Phys. Chem.* **1992**, *96*, 6204–6212.

(41) Lautie, A.; Novak, A. *J. Chim. Phys. Physicochim. Biol.* **1968**, *65*, 1359–1368.

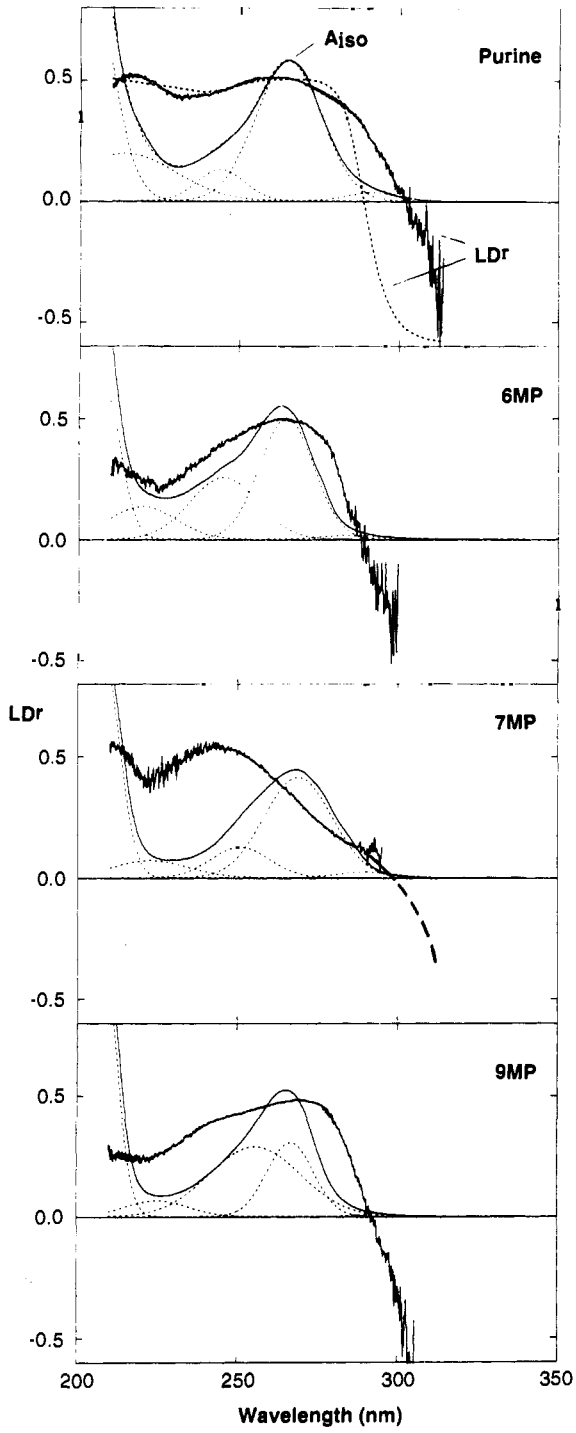

Figure 2. Reduced linear dichroism (LD^r, thick curve) and absorption (A_{iso}, thin curve) spectra resolved into Gaussian components (dashed) of purine, 6-methylpurine, 7-methylpurine, and 9-methylpurine in stretched poly(vinyl alcohol) film. LD^r (scale) and A_{iso} (arbitrary) are calculated from measured $A_\parallel$ and $A_\perp$ spectra, and the Gaussian components are calculated from simultaneous least-squares fit to parallel and perpendicular components. The top panel also shows the LD^r (dashed thick line) and absorption (dashed thin line) spectra calculated from the fitted polarized components for purine. The dashed continuation of the LD^r curve for 7MP represents data taken from measurements on concentrated films.

direction of the orientation axis relative to the pseudo-symmetry long axis of the purine chromophore (angle α counted positive toward N7; see Figure 1) is estimated from the comparison between common vibrational transitions in differently substituted derivatives. For a given vibration, which is not itself affected by a certain substituent, the observed change in transition moment direction relative the orientation axis (angle θ) just corresponds

Table I. IR Polarizations for Purine, 6-Methylpurine, 7-Methylpurine, and 9-Methylpurine

		transition																					
		1	2	3	4	5	6	7	8	9	10	11	12	13	14	15	16	17	18	19	20	21	22
	assgn[a]		1610 Py	1591	1571 Py	1488 Im	1408 Py		1332	1299	1270 δNH	1230 δCH				940 A′	914	806	796 A″		640 A′	609 A″	
purine	ν (cm^{-1})		1610	1588	1568	1488	1404		1332	1298	1271	1232				938	912	804	796		643	611	573
	LD^r		0.45	0.03	0.36	0.3	0.47		0.46	0.6	0.41	0.37				0.12	0.43	−0.72	−0.72		−0.70	−0.70	0.35
	θ (deg)[b]		37	78	44	50	35		36	22	40	43				66	38	90	90		90	90	45
	δ (deg)[c]		+37, −37	+78, −78	+44, −44	+50, −50	+35, −35		+36, −36	+22, −22	+40, −40	+43, −43				+66, −66	+38, −38	oop	oop		oop	oop	+45, −45
6MP	ν (cm^{-1})	1626	1606		1567	1478		1383	1330	1303		1234			965	932	887	804	796		648	612	
	LD^r	0.29	0.45		0.38	0.1		0.0	0.12	0.20		0.36			0.4	0.47	0	−0.69	−0.69		−0.7	−0.7	
	θ (deg)[b]	50	37		43	70		90	66	58		44			40	35	90	90	90		90	90	
	δ (deg)[c]	+30, −70	+17, −57		+23, −63	+50, −90		+70	+46, −86	+48, −78		+24, −64			+20, −60	+15, −55	+70	oop	oop		oop	oop	
7MP	ν (cm^{-1})		1614		1568	1493	1412		1360	1314	1262		1211				915	802		750		610	586
	LD^r		0.05		0.38	0.36	0.7		0.35	0	0.60		0.0				0.19	−0.75		0.51		−0.8	0.60
	θ (deg)[b]		75		45	46	15		47	90	27		90				60	90		34		90	27
	δ (deg)[c]		+90, −60		+60, −30	+61, −31	+30, 0		+62, −32	−75	+42, −12		−75				+75, −45	oop		+49, −19	oop	oop	+42, −12
9MP	ν (cm^{-1})		1603	1584		1515	1406		1348	1308		1235	1213	1199	1051		913		793		642		547
	LD^r		0.53	0.13		0.35	0.4		0.45	0.45		−0.03	0.1	0.06	0.0		0.27		910		90		53
	θ (deg)[b]		25	63		43	36		34	34		0	67	72	90		50		90		90		53
	δ (deg)[c]		+15, −35	+53, −73		+33, −53	+26, −46		+24, −44	+24, −44		−10	+57, −77	+62, −82	+80		+40, −60		oop		oop		+43, −63

[a] Assignments according to Lautié.[41] Py = vibration localized in the pyrimidine moiety; Im = vibration localized in the imidazole moiety. δNH and δCH denote NH and CH in-plane bending modes, respectively; A″ and A′ refer to which irreducible representation the vibration belongs. [b] Angle between IR transition moment and molecular orientation axis. [c] Angle between IR transition moment and the pseudo-symmetry long axis of the purine chromophore.

Table II. UV Transition Moments for Purine, 6-Methylpurine, 7-Methylpurine, and 9-Methylpurine

		transition				
		I	II	III	IV	V
	character	$n\pi^*$	$\pi\pi^*$	$\pi\pi^*$	$\pi\pi^*$	$\pi\pi^*$
purine[a]	λ (nm)	292	265	244	214	200
$3S_{zz} = 0.7$	ε (M^{-1} cm^{-1})[b]	460	7600	1700	2600	15500
$3S_{yy} = 0.0$	LD[r]	−0.7	0.51	0.43	0.46	0.51
$\alpha = 0$	θ (deg)	90	31	38	36	31
	δ (deg)	oop[c]	+31, −31	+38, −38	+36, −36	+31, −31
6MP[a]	λ (nm)	285	265	245	220	208
$3S_{zz} = 0.7$	ε (M^{-1} cm^{-1})[b]	230	7000	3600	1900	10000
$3S_{yy} = 0.0$	LD[r]	−0.7	0.48	0.43	0.15	0.42
$\alpha = 20$	θ (deg)	90	34	38	62	39
	δ (deg)	oop[c]	+14, −54	+18, −58	+42, −82	+19, −59
7MP[a]	λ (nm)	295	269	251	223	208
$3S_{zz} = 0.75$	ε (M^{-1} cm^{-1})[b]	390	6930	2110	1200	15600
$3S_{yy} = 0.0$	LD[r]	−0.75	0.31	0.71	0.48	0.57
$\alpha = +15$	θ (deg)	90	50	13	37	29
	δ (deg)	oop[c]	+65, −35	+28, +2	+52, −22	+44, −14
9MP[a]	λ (nm)	290	267	256	225	207
$3S_{zz} = 0.65$	ε (M^{-1} cm^{-1})[b]	180	4230	4460	950	17600
$3S_{yy} = 0.0$	LD[r]	−0.65	0.52	0.42	0.30	0.27
$\alpha = -10$	θ (deg)	90	27	37	47	50
	δ (deg)	oop[c]	+17, −37	+27, −47	+37, −57	+40, −60

[a] The table comprises data evaluated from Figure 2. λ, ε, and LD[r] are the peak wavelength, molar absorptivity, and reduced linear dichroism, respectively, associatd with each Gaussian component. θ and δ denote angles between electronic transition moment and molecular orientation axis and pseudo-symmetry long axis, respectively. The preferred solutions are underlined. [b] Based on ε (265 nm) = 7600 M^{-1} cm^{-1} for purine.[9] [c] Out-of-plane.

to the change in direction of the orientation axis. For example, knowing that substitution at N9 by a methyl group will turn the orientation axis clockwise (Figure 4) gives the possibility to compare a number of vibrational transition moments (preferably localized in the pyrimidine moiety) and thereby to estimate the relative directions of the orientation axes. We have made an ad hoc assignment of the orientation axis of purine itself to be along the purine pseudo-symmetry long axis (i.e., $\alpha = 0$), motivated by the molecular shape and comparison with similarly shaped molecules such as indole.[39,40] The orientation parameters and directions of orientation axes are collected in Table II.

The molar absorptivities and the reduced linear dichroisms at the respective band maxima, corresponding to the results in Figure 2, are shown in Table II. Transition moment directions relative to the orientation axis (angle θ) are calculated from eq 4 using the estimated orientation parameters. Table II also includes absolute transition moment directions relative the pseudo-symmetry axis defined in Figure 1 (angle δ). For transitions II, III, and IV, the preferred solution for each transition moment direction is underlined. Figure 4 shows directions of the concluded UV transition moments and preferred molecular orientation axes.

Emission Properties. Figure 5 displays phosphorescence emission spectra and anisotropies for purine, 6-methylpurine, 7-methylpurine, and 9-methylpurine in EPA glass at 80 K. All purines studied show weak unstructured or negligible fluorescence ($\Phi_f < 0.001$), but strong and structured phosphorescence ($\Phi_p \approx 1$). The vibrational structure shows a complicated pattern with several progressions. The phosphorescence anisotropy has mainly negative polarization upon excitation at 265 nm ($\pi\pi^*$) but positive upon excitation at 290 nm ($n\pi^*$). The lifetime of the phosphorescence was estimated to be approximately 1.8 s for the main emission intensity of purine and 6MP and for the whole emission spectrum of 9MP. The weak features at approximately 360 nm in purine and 6MP, and the whole emission spectrum of 7MP, show a shorter lifetime close to 0.9 s. Figure 6 shows phosphorescence excitation and absorption spectra in EPA glass at 80 K. For purine and 6MP the shape of the excitation spectra depends strongly on emission wavelength; viz., two components with different absorption and emission spectra (displayed with different lines in Figure 6) are present in these samples at 80 K. 7MP and 9MP do not exhibit any dependence in shape of excitation spectra with emission wavelength. Parameters describing the emission are summarized in Table III.

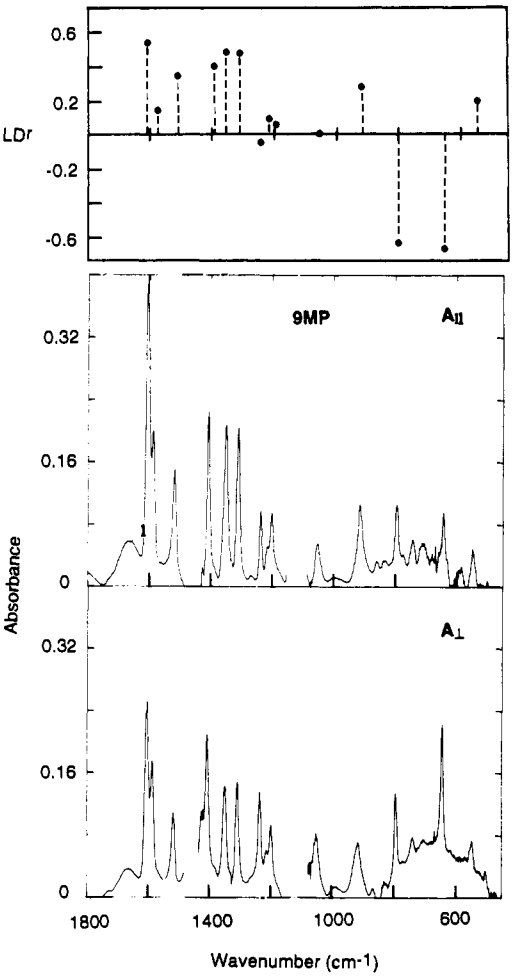

Figure 3. Polarized vibrational spectrum of 9-methylpurine in stretched poly(vinyl alcohol). Top panel shows reduced linear dichroism (LD[r]) values calculated from the polarized components.

Theoretical Calculations. In order to monitor changes upon substitution and to characterize the electronic transitions, we have

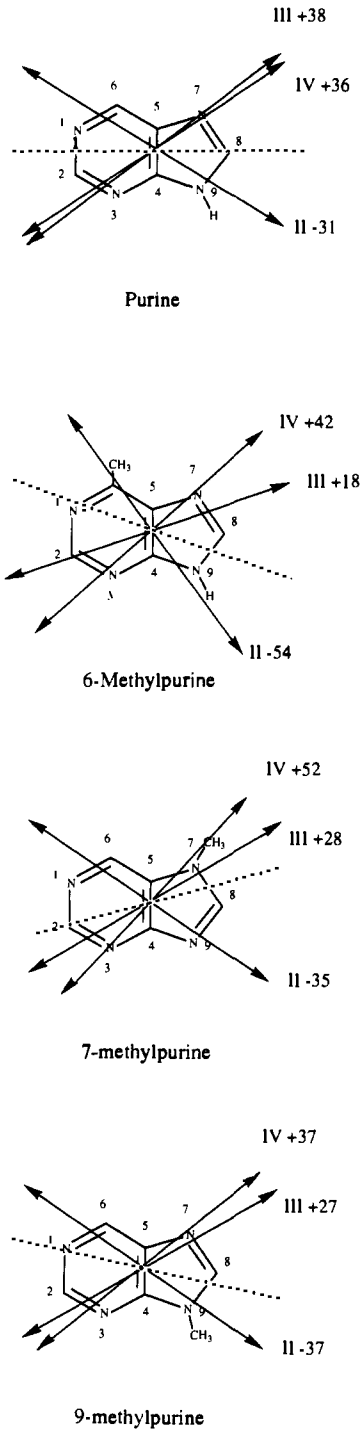

Figure 4. Transition moment directions for the first three in-plane polarized transitions (II, III, and IV) concluded from the present dichroic study. The dashed lines represent the preferred molecular orientation axes. The lengths of the arrows are arbitrary.

performed a number of semiempirical molecular orbital calculations on the excited states of the purine derivatives. Table IV comprises the most important results from these calculations. The $S_0 \rightarrow S_i$ transition energies and oscillator strengths were generally found to agree fairly well with the experimental results, at least for the $\pi \rightarrow \pi^*$ transitions. However, the transition moment directions were for some transitions sensitive to the size of the CI basis set which is why they should be considered only as rough estimates.

Discussion

In order to characterize the electronic absorption spectrum of a molecule, we need information about number and nature of the transitions, their energies, intensity distributions, and transition

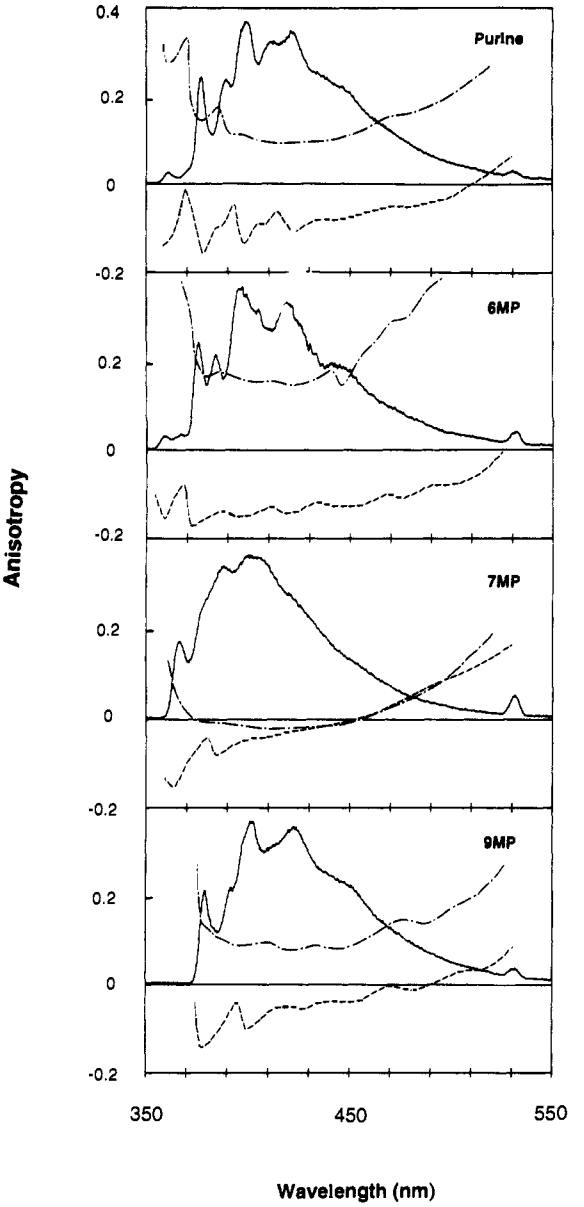

Figure 5. Phosphorescence (—, excited at 265 nm) and phosphorescence anisotropy (- - -, excited at 265 nm, ---, excited at 290 nm) spectra of purine, 6-methylpurine, 7-methylpurine, and 9-methylpurine in EPA glass at 80 K. The "peak" at 530 nm is due to scattered light passing the monochromator grating at double the excitation wavelength.

moment directions. Often such information originates from different sources such as polarized spectroscopy on crystals or other ordered systems, solvent effects on normal absorption spectra, luminescence properties (including anisotropy), magnetic and normal circular dichroism (MCD and CD), and quantum mechanical calculations. A natural starting point is to establish number and nature of electronic transitions contributing to the UV spectrum.

The strongly negative LD observed at the red edge of the first absorption band of all purines (Figure 2) strongly suggests the existence of an out-of-plane polarized transition. The influence of base-line errors was eliminated by also measuring on 10 times more concentrated films in the 290-nm region giving accurate LD^r values for the negative LD signal. As seen in Figure 2 (top panel), the reduced linear dichroism calculated from the fitted polarized absorption spectra matches fairly well the experimental LD^r curve over the main absorption bands. There is, however, an apparent misfit in LD^r at the red edge of the 265-nm band. A highly plausible explanation for this deviation is that the effective polarization of the $n \rightarrow \pi^*$ transition is not constant over the absorption band but varies as a result of vibronic coupling. Closer

Table III. Data Comprising the Phosphorescence Spectra of Purine, 6MP, 7MP, and 9MP in EPA Glass at 80 K

		$\lambda(T_1 \rightarrow S_0)^a$ (nm)	$\Delta E(T_1-S_1)^b/cm^{-1}$	$\Phi_p{}^c$	$\tau_p{}^d$ (s)	$\tau_{0p}{}^e$ (s)
purine	minior[f]	360.5	6500		0.7	(0.8)
	major[f]	377.3	7740	0.9 ± 0.1	1.5	1.7
6MP	minor[f]	359.1	6600		0.9	(0.9)
	major[f]	375.9	8480	1.0 ± 0.1	1.8	1.8
7MP		366.5	6610	1.0 ± 0.1	0.9	0.9
9MP		379.1	8100	0.8 ± 0.1	1.1	1.4

[a] Wavelength of the 0,0 $T_1 \rightarrow S_0$ transition. [b] Energy difference between T_1 and S_1 state measured as the difference between $S_0 \rightarrow S_1$ absorption energy and the 0,0 energy of the phosphorescence spectra. [c] Phosphorescence quantum yield based on $\Phi_f = 1.0$ for 9,10-diphenylanthracene in EPA at 80 K. [d] Estimated mean lifetime of phosphorescence. [e] Natural phosphorescence lifetime calculated as $\tau_{0p} = \tau_p/\phi_p$. [f] Major and minor denotes the major (9H) and minor (7H) tautomeric forms of purine and 6MP (see text).

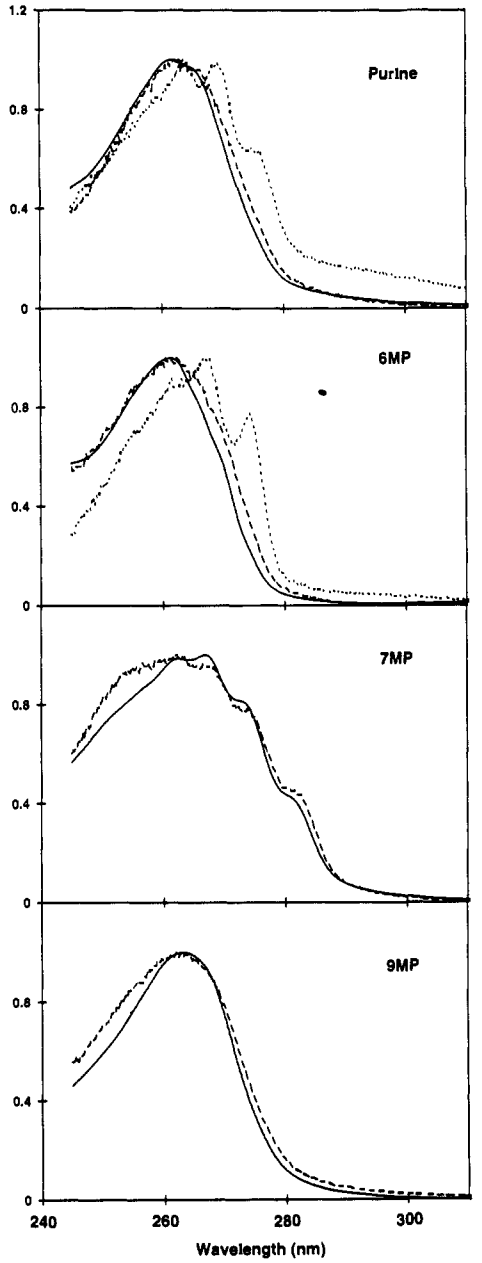

Figure 6. Absorption (—) and phosphorescence excitation spectra for the major (---, λ_{em} = 400 nm) and minor (···, λ_{em} = 360 nm) emitting components in EPA glass at 80 K (arbitrary ordinate scale). 7MP and 9MP behave as single components, and no variation in excitation spectra band shape with emitting wavelength was detected. The intensity in the minor component above 300 nm is due to insufficient subtraction of fluorescent impurities in the solvent.

to the much stronger in-plane polarized transitions, more intensity is borrowed from these by the $n \rightarrow \pi^*$ vibronic transitions whose polarization then acquires more in-plane character. The other compounds (6MP, 7MP, and 9MP) show similar behavior, but

Table IV. Calculated[a] Transition Wavelengths (λ), Oscillator Strengths (f), and Moment Directions (δ) for Purine, 6-Methylpurine, 7-Methylpurine, and 9-Methylpurine

		transition[b]			
		purine	6-methyl-purine	7-methyl-purine	9-methyl-purine
1 $n\pi^*$ I	λ ($S_0 \rightarrow S_1$)[c]	317	309	342	320
	f	0.017	0.013	0.013	0.014
	δ[d]	oop	oop	oop	oop
	λ ($S_0 \rightarrow T_i$)[e]	317	309	342	320
2 $\pi\pi^*$ II	λ ($S_0 \rightarrow S_2$)[c]	290	290	291	290
	f	0.024	0.011	0.028	0.018
	δ[d]	-29	-58	-28	-31
	λ ($S_0 \rightarrow T_1$)[e]	488	495	442	482
3 $n\pi^*$	λ ($S_0 \rightarrow S_3$)[c]	286	283	298	290
	f	0.032	0.020	0.006	0.044
	δ[d]	oop	oop	oop	oop
	λ ($S_0 \rightarrow T_i$)[e]	286	283	298	290
4 $n\pi^*$	λ ($S_0 \rightarrow S_4$)[c]	264	264	281	269
	f	0.044	0.045	0.084	0.033
	δ[d]	oop	oop	oop	oop
	λ ($S_0 \rightarrow T_i$)[e]	264	264	281	269
5 $\pi\pi^*$ III	λ ($S_0 \rightarrow S_5$)[c]	259	266	264	264
	f	0.142	0.17	0.114	0.106
	δ[d]	-7	-13	+24	-16
	λ ($S_0 \rightarrow T_i$)[e]	402	400	408	397
6 $n\pi^*$	λ ($S_0 \rightarrow S_6$)[c]	238	238	238	240
	f	0.011	0.014	0.000	0.009
	δ[d]	oop	oop	oop	oop
	λ ($S_0 \rightarrow T_i$)[e]	238	238	238	240
7 $\pi\pi^*$ IV	λ ($S_0 \rightarrow S_7$)[c]	224	226	224	228
	f	0.139	0.102	0.169	0.215
	δ[d]	+33	+37	-36	+29
	λ ($S_0 \rightarrow T_i$)[e]	368	369	366	365
8 $\pi\pi^*$ V	λ ($S_0 \rightarrow S_8$)[c]	207	210	214	212
	f	0.224	0.284	0.249	0.209
	δ[d]	+40	+46	+7	+8
	λ ($S_0 \rightarrow T_i$)[e]	331	322	328	331
9 $\pi\pi^*$	λ ($S_0 \rightarrow S_9$)[c]	200	201	204	204
	f	0.285	0.238	0.235	0.213
	δ[d]	-40	-28	+47	-68
	λ ($S_0 \rightarrow T_i$)[e]	27	288	287	284

[a] CNDO/S calculation with Mataga–Nishimoto electron repulsion integral and 20 singly excited configurations in the CI calculation. [b] The identification of corresponding observed transition is made by Roman numbers. [c] Wavelength (in nm) for singlet–singlet transitions. The order of the transition energies may vary between the different derivatives. [d] Transition moment direction relative molecular long axis (see Figure 1). [e] Wavelength (in nm) for singlet–triplet transitions.

the computed LD^r curves are left out for clarity reasons.

The main intensity of the 260-nm band is due to two $\pi \rightarrow \pi^*$ transitions. Because of the relative orientation of their transition moments and the orientation axis, purine itself displays only a moderate wavelength dependence in LD^r over the 260-nm band (Figure 2). By contrast, 7-methylpurine shows a pronounced variation of LD^r with wavelength because the transition moments in this case are differently projected on the rotated orientation axis (Figure 4). Magnetic circular dichroism (MCD) measurements[42] and solvent shifts in absorption spectra[9] also suggest two

(42) Townsend, L. B.; Miles, D. W.; Manning, S. J.; Eyring, H. *J. Heterocycl. Chem.* **1973**, *10*, 419–421.

differently polarized $\pi \rightarrow \pi^*$ transitions in this region. The second absorption band at 205 nm is hard to analyze because of instrumental limitations. With current equipment we cannot measure polarized spectra below 210 nm, and therefore only the red edge of the 205-nm band is covered in the analysis. Still, in order to accurately fit the polarized components, at least two in-plane polarized transitions are required to be located in this region.

The intensity distribution and transition moment directions are intimately connected. We have therefore chosen to fit the two independent polarized absorption spectra simultaneously in order to include both the absorption features (peaks, shoulders, etc.) and the polarization information in the analysis. The choice of Gaussian profiles is, of course, arbitrary but works as well as any other (e.g., Lorentzian) when fitting broad unstructured condensed-phase spectra. We have also tried to fit the spectra on a wavenumber basis (linear in energy) with insignificant deviations from the wavelength-based results. The reduced linear dichroism evaluated from the amplitudes of the parallel and perpendicular Gaussian components are compared with the experimental LD^r curve to ensure consistency. The accuracy of the transition moment directions rely on the quality of the orientation determination as well as on the accuracy of the measured LD^r values. The in-plane orientation parameters are subject to some uncertainty since they are estimated as the limiting values of the observed IR LD^r values. This uncertainty may have large effect on transition moments oriented near parallel or near perpendicular to the orientation axis (i.e., with LD^r values close to $3S_{zz}$ or $3S_{yy}$), while its influence on transition moments oriented in between these extremes is small. Fortunately, the UV transition dipoles in purine and its methyl derivatives are oriented with, in this context, "favorable" angles to the orientation axes (the second observed $\pi \rightarrow \pi^*$ transition in 7MP is an exception). Evidently, the determination of orientation axes directions also influences the final result. With all parts considered, we estimate the accuracy of the UV transition moment directions in Table II and Figure 4 to be within $\pm(5-10)°$, where the larger number refers to the transition of the high-energy band.

Chen and Clark have determined the UV transition dipole moments for crystals of purine[13] and found evidence for an out-of-plane polarized transition at 293 nm and the first $\pi \rightarrow \pi^*$ transition at 263 nm to be polarized −42° to the long axis, in accordance with our results. However, our second $\pi \rightarrow \pi^*$ transition in the 260-mm absorption band (transition III) lacks counterpart in Chen and Clark's work (they place an $n \rightarrow \pi^*$ at 250 nm and a weak $\pi \rightarrow \pi^*$ transition at 230 nm). They further conclude that the strong second band is composed of an in-plane transition (at 200 nm) polarized −40° to the long axis and a strong $n \rightarrow \pi^*$ transition (at 190 nm). Thus, our negatively polarized solution for transition V is consistent with Clark's results.

Purine Phosphorescence. The phosphorescence of the methyl derivatives of purine are similar to the purine phosphorescence with almost unit quantum yields and observed lifetimes around 1–2 s. This corresponds to a radiative rate constant, k_p, for the $T_1 \rightarrow S_0$ process of 0.5–1 s^{-1}. The singlet triplet splitting is between 6500 and 8500 cm^{-1} measured as the difference between the red edge of the absorption spectrum and the (0,0) peak of the phosphorescence spectrum. These two results point unequivocally toward a $^3(\pi\pi^*)$ assignment for the emitting triplet state.[43] According to *empirical* rules[44] the phosphorescence from a $^3(\pi\pi^*)$ state is expected to be out-of-plane polarized due to first-order (i.e., direct) spin–orbit coupling to $^1(n\pi^*)$ states. The mechanism suggests that some singlet character is mixed into the lowest triplet state by interaction with a close-lying singlet $n\pi^*$ state. Upon excitation at 265 nm we observe large negative anisotropies at the origin of the phosphorescence, thus indicating that the absorbing and emitting transition dipoles are perpendicular to each other. Excitation at 290 nm, i.e., the $n \rightarrow \pi^*$ transition, yields positive anisotropy at the origin (Figure 5). Both these polarization observations are thus consistent with the proposed out-of-plane polarized $T_1 \rightarrow S_0$ transition.

With increasing emission wavelengths (corresponding to transitions that end in higher vibronic components of the electronic ground state), an oscillation as well as a rise in anisotropy (265-nm excitation) is seen. This indicates that another, differently polarized emission contributes at higher wavelengths. The negative "peaks" in anisotropy correspond to intensity peaks in the phosphorescence spectra. Similar behavior has been observed for other aromatic[45,46] and heteroaromatic[44] molecules and has been rationalized by inclusion of second-order spin–orbit coupling.[47] Here the emitting $^3(\pi\pi^*)$ state is vibronically coupled to a $^3(n\pi^*)$ state which in turn is spin–orbit coupled to a $^1(\pi\pi^*)$ state. Since the phosphorescence is spin forbidden, the polarization of the phosphorescence is dictated by the lending singlet–singlet transition and, thus, is in-plane polarized for the second-order mechanism here described. The second-order spin–orbit coupling is generally expected to be of less importance than the direct coupling, but in certain cases it could contribute significantly. Despite the fact that the coupling matrix elements are orders of magnitude smaller for the second-order, compared to the first-order mechanism, the oscillator strengths for the lending transitions, on the other hand, differ by a factor of 50 in favor of the indirect mechanism. Phosphorescence anisotropy measured with excitation at 290 nm also shows some variation in anisotropy at the higher emission wavelength, as expected, but rises to a large positive value at the red edge of the band, a fact that is not accounted for by the proposed mechanism and the origin of which is not presently understood.

In summary, purine and its three methyl derivatives have phosphorescence spectra that indicate a $^3(\pi\pi^*)$ emitting triplet state. The polarization properties suggest that it borrows singlet character by direct spin–orbit coupling from a nearby $^1(n\pi^*)$ state and, as well, by second-order spin–orbit coupling to $^1(\pi\pi^*)$ states via a $^3(n\pi^*)$ state vibronically coupled with the $^3(\pi\pi^*)$ state. Evidence for a similar behavior has also been reported for the purine phosphorescence by Drobnik et al.,[12] and they accordingly assigned the emitting triplet to have $^3(\pi\pi^*)$ character.

Tautomerism in Purine? The phosphorescence emission spectra of all purines studied show a complicated vibrational structure (Figure 5). The spectra are all very similar with almost coinciding vibronic progressions, apart from the weak features at the blue-end side of the main emission intensity in purine and in 6-methylpurine. The latter feature was assigned as the (0,0) transition for purine by earlier investigators.[8,9] Its absence in 7-methylpurine and 9-methylpurine led us to believe that it could instead be due to a ground-state heterogeneity involving the imidazolic hydrogen, i.e., 7H–9H tautomerism. The phosphorescence excitation spectra corresponding to these weak features are structured and thus very different from the absorption spectra, in contrast to the bulk of the excitation spectra which is unstructured and has approximately the same spectral band shape as the absorption spectra (Figure 6). The band shape of the excitation spectra for 7MP and 9MP, on the other hand, is independent of emission wavelength, indicating that these compounds behave as single ground-state species. Furthermore, the phosphorescence mean lifetime for the weak features differs from the rest of the spectrum (Table III). To summarize, we have indications that purine and 6MP in EPA glass at 80 K both consist of one major component with unstructured absorption and long-lived phosphorescence, and one minor component with structured, slightly red-shifted absorption and more short-lived, blue-shifted phosphorescence. In contrast, 7- and 9-methylpurine behave as single spectroscopic species.

We interpret these purine components as the 9H (major) and 7H (minor) tautomers based on the following arguments. The *minor* component in purine and 6MP (in EPA at 80 K) possesses the following properties: (1) vibrationally structured, slightly

(43) Turro, N. J. *Modern Molecular Photochemistry*; Benjamin Cummings Publishers: Menlo Park, CA, 1978; Chapter 5.
(44) El-Sayed, M. A.; Brewer, R. G. *J. Chem. Phys.* **1963**, *39*, 1623–1628.
(45) El-Sayed, M. A.; Pavloupolus, T. *J. Chem. Phys.* **1963**, *39*, 1899–1900.
(46) Pavloupolus, T.; El-Sayed, M. A. *J. Chem. Phys.* **1964**, *41*, 1082–1092.
(47) Lim, E. C.; Yu, J. M. H. *J. Chem. Phys.* **1967**, *47*, 3270–3275.

red-shifted absorption and phosphorescence excitation spectra; (2) natural phosphorescence lifetimes close to 0.9 s; and (3) slightly blue-shifted phosphorescence spectra, relative to the (0,0) peak in purine, a fact that is accounted for by the relative triplet energies obtained from the CNDO/S calculation (Table IV). The same properties are observed with 7MP which behaves as a single species.

The *major* component in purine and 6MP has the following properties: (1) unstructured absorption and phosphorescence excitation spectra with similar band shapes and peak wavelengths; (2) natural phosphorescence lifetime close to 1.8 s; and (3) almost coinciding phosphorescence spectra. The same properties are observed with 9MP which behaves as a single species.

These observations strongly indicate that 7- and 9-methylpurine represent model chromophores for respectively the 7H and 9H tautomers of purine and 6-methylpurine. The relative amount of the minor component (7H) is estimated from the absorption and phosphorescence spectra to be not more than 5% in both purine and 6MP in EPA at 80 K. The amount of 7H tautomer *decreases* with *increasing* temperature as judged from the temperature dependence of the absorption (EPA) and phosphorescence (propylene glycol) spectra (results not shown).

The influence from different tautomeric forms of the purines on their spectra measured in PVA hosts is hard to judge, and the polarized spectra for purine and 6MP are analyzed as if due to a single species (9H). This treatment can be at least partly justified by the following arguments. Firstly, neither the UV nor the IR spectra in PVA at room temperature show any anomalous features such as broadened or extra bands when comparing purine and 6MP with the single-species compounds 7MP and 9MP. Secondly, the results from the low-temperature EPA spectra indicate only small amounts (less than 5%) of 7H tautomer, decreasing with higher temperature. In fact, the absorption band shape is only slightly affected by changing the temperature from room temperature to 80 K for both purine and 6MP in EPA. Thirdly, the results obtained from the polarized measurements, i.e., resolved transition band envelopes and moment directions, are consistent when comparing all four compounds studied.

Molecular Orbital Calculation. A prerequisite for a meaningful comparison of theoretical and experimental results is that a correct assignment between calculated and observed transitions can be made. Since the $n \rightarrow \pi^*$ transitions are weak, we only observe the lowest one at the red edge of the 260-nm band. The other higher lying $n \rightarrow \pi^*$ transitions (calculated transitions no. 3, 4, and 6) are hidden by much stronger $\pi \rightarrow \pi^*$ transitions and could, thus, not be observed by the LD measurements. The discussion is therefore confined to the first $n \rightarrow \pi^*$ transition and the four lowest $\pi \rightarrow \pi^*$ transitions (calculated transitions 1, 2, 5, 7, and 8).

The transition energies are generally calculated too low. This is particularly obvious for the $S_0 \rightarrow T_1$ transitions of $\pi\pi^*$ character presumably because the parameters used in the calculation are not optimized for singlet–triplet transitions (the $S_0 \rightarrow T_1$ transition wavelength can be estimated from the (0,0) band of the phosphorescence spectrum). The calculated oscillator strengths for the $n \rightarrow \pi^*$ transitions are a factor 10 larger than observed, in contrast to the first $\pi \rightarrow \pi^*$ transition where the oscillator strength is instead calculated too small. Comparing different compounds the largest effect is seen upon methylation in the 7th position. This is because substituting in the 9th and 6th position of the purine chromophore only exchanges a hydrogen for a methyl group, whereas in 7-methylpurine the location of the n-electrons as well as the position of the double bond in the imidazole ring are changed. These alterations in electronic structure lower the energy for the $n \rightarrow \pi^*$ transition (transition 1) and changes the transition moments significantly for transition 5 and 7. None of these predicted properties are readily observed in the spectrum of 7-methylpurine. However, the energy for the $S_0 \rightarrow T_1$ transition (transition 2) is higher for 7MP than for derivatives with the 9th position substituted, which is consistent with the relative 0,0 energies obtained from the phosphorescence spectra. In conclusion, whereas the CNDO/S calculation provides consistent information about the number of electronic transitions and their relative energies, it fails in some cases to predict directions of transition moments.

Conclusions

Purine, 6-methylpurine, 7-methylpurine, and 9-methylpurine all exhibit an isolated $n \rightarrow \pi^*$ transition around 290 nm and $\pi \rightarrow \pi^*$ transitions at approximately 265, 244, and 215 nm. These $\pi \rightarrow \pi^*$ transitions are polarized at, respectively, −31°, +38°, and +36° relative to the pseudo-symmetry long-axis in purine, and show only small deviations for the methyl derivatives. The purines show strong phosphorescence, with nearly unit quantum yield, and the emitting triplet state is assigned to have effectively $\pi\pi^*$ character. Purine and 6-methylpurine display characteristics of a prototropic tautomerism in EPA glass at 80 K, and the phosphorescence excitation spectra (i.e., effectively the absorption spectra) for the tautomers are isolated. The tautomers are identified as 7H- and 9H-purine.

Acknowledgment. Dr. Mikael Sundahl is greatly acknowledged for supervising the synthesis of 7- and 9-methylpurine. We are grateful for illuminating discussions with Dr. Kjell Sandros. This project is supported by the Swedish Natural Science Research Council.

Registry No. 6MP, 2004-03-7; 7MP, 18346-04-8; 9MP, 20427-22-9; purine, 120-73-0.